Synthesis, Characterization And Biological Studies Of Metal (II) – Cinnamaldehyde-4,4'-Diaminodiphenylmethane

Ezhil Arasi R[1*] and Dr. Kalaikathir S P R[2]

[1*]Research scholar, Reg.No.20223282032004, Department of chemistry and Research Centre, Women's Christian College, Nagercoil-1. (Affiliated to Manonmaium Sundaranar University, Tirunelveli), Email:arasi1920@gmail.com.
[2]Associate Professor, Department of chemistry and Research Centre, Women's Christian College, Nagercoil-1. (Affiliated to Manonmaium Sundaranar University, Tirunelveli), Email:kalaikathirspr@gmail.com

[*]**Corresponding Author:** Ezhil Arasi R
*Research scholar, Reg.No.20223282032004, Department of chemistry and Research Centre, Women's Christian College, Nagercoil-1.

ABSTRACT
A new Schiff base ligand was derived from the condensation reaction of Cinnamaldehyde and 4, 4'-diaminodiphenylmethane. Using this ligand the transition metal complexes Cu (II), Zn (II), Co (II) and Ni (II) were synthesized. The structural features of the synthesized compounds were confirmed by UV visible, NMR spectroscopic techniques and SEM. The thermal behavior of the metal complexes was determined by thermo gravimetric analysis (TGA). All the metal complexes were investigated for their anti oxidant and anti inflammatory activity. The metal complexes were tested the larvicidal activity against Culexquinquefaciatus. Anticancer activities were also studied towards human Osteosarcoma cells. Molecular docking also studied for the ligand and metal complexes. The obtained result showed that the complexes especially Cu (II) metal complex strongly active against cancer cells.

Key Words: Schiff base, Molecular docking, larvicidal activity, anticancer activity.

INTRODUCTION

The chemistry of transition metal complexes has been receiving considerable current attention, because of the interesting biological properties exhibited by these complexes. Transition metal complexes have useful applications in the biological field. Several complexes of multidentate ligands containing O and N donor sites were used for catalysis. In comparison with other transition metal complexes, transition metal complexes also have many chemical and industrial applications. Metal complexes of Schiff bases derived from diaminodiphenylmethane derivatives are used for their wide range applications in agro industry, catalysis, and biological activities have been reported widely (Rezaeivala and Keypour 2014) Similarly, cinnamaldehyde derivatives are of great interest. Synthesis and characterization of ligand derived from cinnamaldehyde with 4,4'-diaminodiphenylmethane and its Co(II), Ni(II), Cu(II) and Zn(II) complexes have been chosen for investigation. Molecular docking, *in vitro* antimicrobial and cytotoxicity activities have also been carried out in order to ascertain their therapeutic values.

2. EXPERIMENTAL

2.1. Materials and methods

All chemicals and solvent were obtained from commercial sources and were used as received without any further purification.

2.2. Synthesis of ligand and complexes

2.2.1. Schiff base Ligand (DC)

Ethanolic solution of 4,4 diamino diphenyl methane and cinnamaldehyde were taken in RB flask in 1:1 molar ratio and refluxed for one hour. The reaction mixture is poured into ice; a yellow compound of Schiff base ligand was obtained. The precipitate was filtered, washed with water and dried. T*he synthetic route is given* below *(Scheme 2.1).*

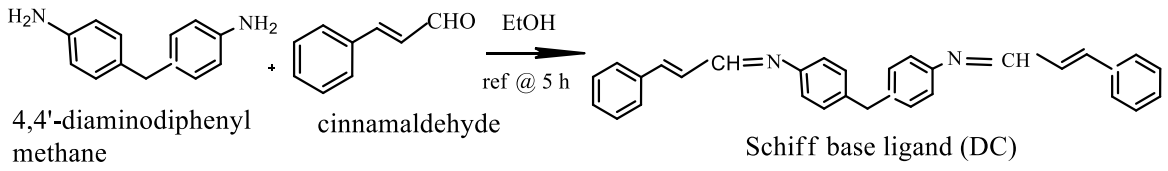

Scheme 2.1. Preparation of DC.

2.2.2 Metal complexes [M(II)-(DC)$_2$]

The metal complexes were prepared by adding ethanolic solution of Zn(II) nitrate, Co(II) nitrate, Ni(II) nitrate and Cu(II) nitrate to the ligand in ethanol in 1:2 (metal: ligand) molar ratio and refluxed for about 12 hours at 80 ºC. The precipitate solid were filtered and washed with ethanol and dried.

The designed novel synthetic route is shown in Scheme 2.2. The designed synthetic route is highly efficient and gave the final compounds in good yields.

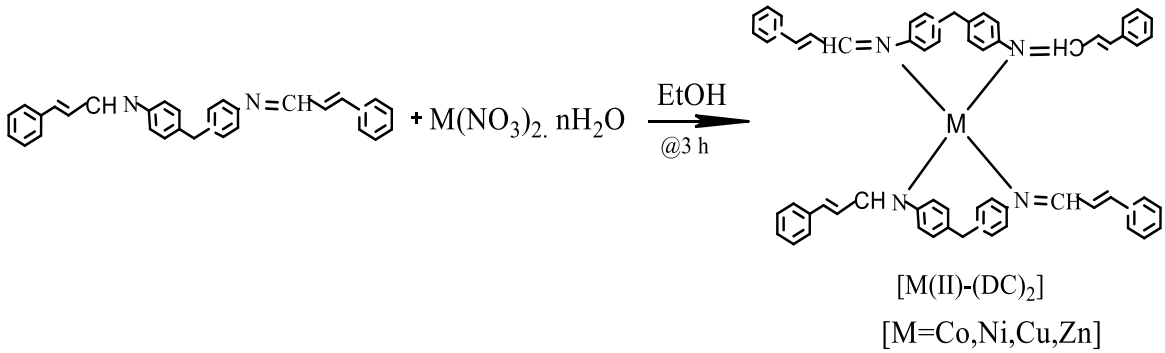

[M(II)-(DC)$_2$]

[M=Co,Ni,Cu,Zn]

Scheme 2.2. Preparation of [M (II)-(DC)$_2$].

2.3. Determination of antimicrobial activity

The agar well diffusion method was used to screen the anti-microbial (20ml) was poured in to each Petri plates. The plates were allowed to solidify for 5minutes and 100µl in Colum suspension was swapped uniformly and allowed to dry for15 minutes. Using sterile cork borer of 8 mm diameter, wells were bored into the seeded agar plates and these were located with a 100 µl solution of each compound in DMSO and all plates were incubated at 37ºC and the diameter of inhibition zone around each disc was measured after 24 hours for bacterial and fungal species. The inhibition zone was developed at which the concentration was noted and the results were recorded from the results, the activity index was calculated.

2.4. Larvicidal activity

The mosquito larvae were collected from water habitats of Nagercoil, Kanyakumari District using a wide mouth container. The mosquito samples were brought to the laboratory, morphologically identified using standard manual and used for larvicidal activity studies. Cleaned sterile beakers were taken and 20 early in star larvae of Culex were taken in 100 ml of tap water. To this 100 ppm of synthesized complexes was added. 20 larvae taken in tap water (without copper complex) served as control. The beakers were kept for 24 h, 48 h, 72 h and 96 h for mortality of the larvae (Culex).

2.5. Anti-inflammatory activity

The reaction mixture (0.5 ml) consisted of 0.45 ml bovine serum albumin (3% aqueous solution) and varying concentration of compound (25, 50, 75,100 µg/ml of final volume), pH was adjusted to 6.3 using small amount of 1N hydrochloric acid. The samples were incubated at 37ºC for 20 min and then heated at 80ºC for 2min. After cooling the samples, 2.5 ml phosphate buffer saline (pH 6.3) was added to each tube. The absorbance was measured using spectrophotometer at 416nm. The percentage inhibition of protein denaturation was calculated as follows:

Percentage inhibition = [(Abs Control – Abs Sample) / Abs control)] x100

2.6. Anti-oxidant activity by dpph radical scavenging assay

Ascorbic acid was used as a reference standard and dissolved in distilled water to make the stock solution with the concentration (1mg/1000µl). The solution of DPPH in methanol 60µM was prepared fresh daily before UV measurements. This solution (3.9ml) was mixed with various concentrations (250, 500, 750, &1000µ*L*). The samples were kept in the dark for 15 minutes at room temperature and the decrease in absorbance was measured at 515nm. Control sample was prepared containing the same volume without any extract and reference ascorbic acid. 95% methanol was used as blank.

Radical scavenging activity was calculated by the following formula.

%Inhibition =(Absorbance of control at 0 minute-Absorbance of Test)/Absorbance of control at 15 minutes x 100

Where C = absorption of control sample (t = 0 min), C= absorption of control (t = 15 min), T = absorption of test solution.

3. RESULTS AND DISCUSSION

3.1 Characterization Studies

3.1.1 Characterization of ligand and its complexes

The purity of DC and complexes were examined by thin layer chromatography. They are readily soluble in EtOH and DMF, while complexes were insoluble in water. All the complexes were stable at RT. The physical parameters of DC and complexes are tabulated in Table 3.1

Table 3.1 Physical and molar conductance data of DC and complexes.

Compounds	**Molecular formula**	**Colour**	**Yield (%)**	**M.P (˚C)**	**Molar conductance ($\Omega^{-1}cm^2mol^{-1}$)**
DC	$C_{31}H_{26}N_2$	Brownish Yellow	87	210	-
[Co(II)-$(DC)_2$]	$C_{62}H_{56}N_4Co$	Purple	81	>300	11
[Ni(II)-$(DC)_2$]	$C_{62}H_{56}N_4Ni$	Green	77	>300	13
[Cu(II)-$(DC)_2$]	$C_{62}H_{56}N_4Cu$	Blue	81	>300	16
[Zn(II)-$(DC)_2$]	$C_{62}H_{56}N_4Zn$	Colourless	80	>300	21

3.1.2. Elemental analysis

Analytical data of DC and complexes are tabulated in Table 3.2. Newly synthesized DC and its [M(II)-$(DC)_2$] showed 1:2 metal-to-ligand stoichiometry for all complexes and in agreement with the elemental analysis data.

Table 3.2. Analytical data of DC and complexes.

Compounds	**Found (Cal.) (%)**		
	C	**H**	**N**
DC	78.00(78.15)	6.09(6.10)	6.49(6.57)
[Co(II)-$(DC)_2$]	81.02(81.62)	5.07(5.70)	6.03(6.14)
[Ni(II)-$(DC)_2$]	81.02(81.62)	5.11(5.70)	6.01(6.14)
[Cu(II)-$(DC)_2$]	81.60(81.65)	5.19(5.70)	6.11(6.14)
[Zn(II)-$(DC)_2$]	81.61(81.65)	5.18(5.70)	6.06(6.14)

3.1.3. Molar conductance

Physical and molar conductance data of DC and complexes are given in Table 3.1. The molar conductance measurements of metal complexes in10^{-3}M DMSO solution were measured. The low molar conductance values the range 11-21 $\Omega^{-1}cm^2mol^{-1}$ suggest the non-electrolytic behavior of complexes (Geary 1971).

3.1.4. Infrared spectra

The important infrared spectral bands of ligand and complexes are given in Table 3.4. IR spectra of DC and [Co(II)-$(DC)_2$], [Ni(II)-$(DC)_2$], [Cu(II)-$(DC)_2$] and [Zn(II)-$(DC)_2$] complexes are shown in Fig 3.4.1-3.4.5 respectively.

IR spectrum of the ligand revealed the absence of characteristic bands of amino group of 4,4'-diaminodiphenylmethane and carbonyl group of thiophene-2-carboxaldehyde fragments of precursors and appearance of a new strong band at 1630 cm^{-1}, which is the characteristic of azomethine group ν(C=N), that confirmed the formation of proposed Schiff base ligand (Mohamed *et al*. 2005).

[Co(II)-$(DC)_2$]

The IR spectrum of DC show a strong band at 1630 cm^{-1} is assigned to stretching vibration of (C=N). During complex formation this azomethine band was shifted to 1633 cm^{-1} indicate coordination of azomethine nitrogen atom to metal ion, which was further evidenced by the appearance of medium intensity band at 444 cm^{-1} due to ν(M-N) vibration [Baradie *et al*., 2014].

[Ni(II)-$(DC)_2$]

A strong band observed at 1630 cm^{-1} in the IR spectrum of DC is assigned to ν(C=N) vibration. This band was shifted to the lower region 1635 cm^{-1} indicate coordination of azomethine nitrogen atom to Ni(II) ion. It was further evidenced by the appearance of medium intensity band at 484 cm^{-1} due to ν(M-N) vibrations.

[Cu(II)-$(DC)_2$]

In the IR spectrum of DC, a strong band observed at 1630 cm^{-1} is assigned to ν(C=N) vibration. This band was shifted to 1635 cm^{-1} in [Cu(II)-$(PT)_2$] suggest coordination of azomethine nitrogen atom to Cu(II) ion. Moreover, medium intensity band appeared at 480 cm^{-1} is assigned to ν(M-N) vibrations.

[Zn(II)-$(DC)_2$]

A strong band at 1630 cm^{-1} in the IR spectrum of DC is assigned to (C=N) stretching vibration. During complex formation this band was shifted to the lower wave number 1640 cm^{-1} point out the involvement of azomethine nitrogen atom in coordination. The appearance of band at 487 cm^{-1} due to ν(M-N) vibrations, this further supports the above observation.

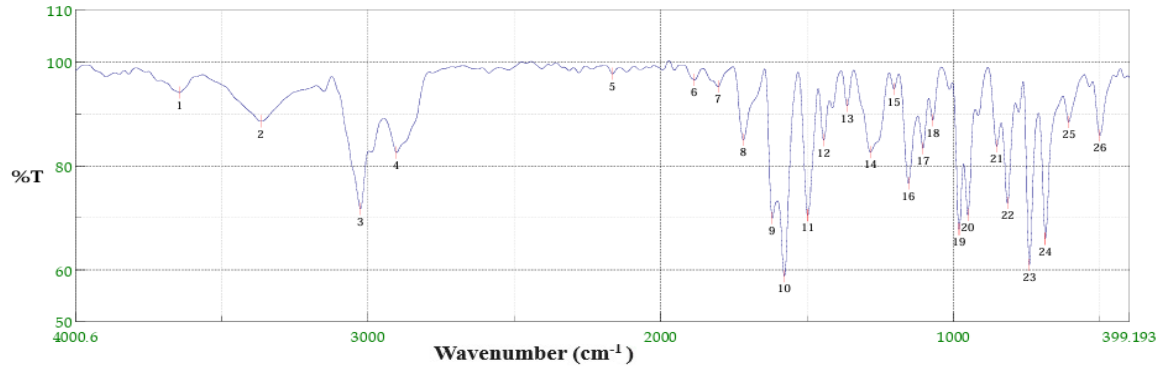

No.	cm-1	%T	No.	cm-1	%T	No.	cm-1	%T	No.	cm-1	%T	No.	cm-1	%T
1	3643.84	94.143	2	3367.1	88.5859	3	3026.73	71.7524	4	2903.31	82.6182	5	2165.67	97.7417
6	1885.08	96.5723	7	1805.04	95.2858	8	1718.26	85.0455	9	1630.91	69.9543	10	1578.45	58.7699
11	1498.42	70.4903	12	1444.42	84.9964	13	1363.43	91.6197	14	1284.36	82.6401	15	1204.33	94.8372
16	1155.15	76.6271	17	1105.01	83.4341	18	1071.26	88.8292	19	981.589	67.8416	20	951.698	70.5932
21	853.346	83.8181	22	815.741	72.8754	23	741.495	60.9594	24	686.534	66.0062	25	606.503	88.4706
26	500.437	85.8985												

Fig. 3.4.1. IR spectrum of DC.

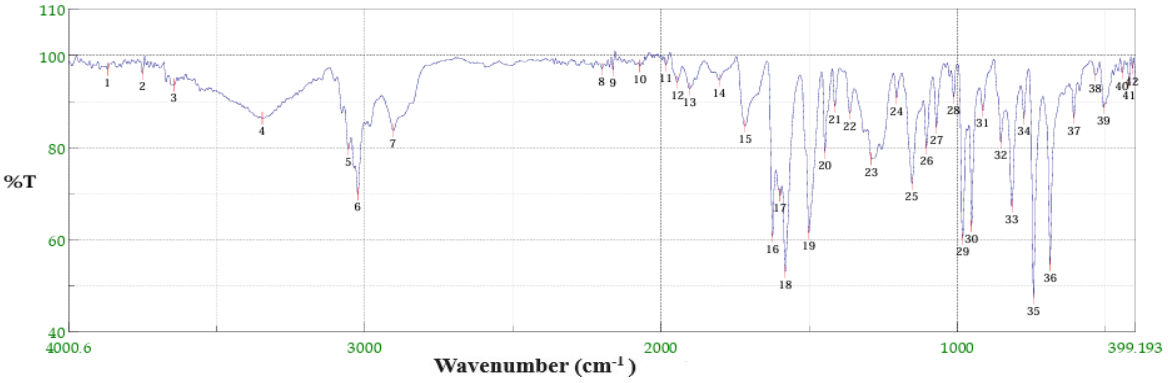

No.	cm-1	%T	No.	cm-1	%T	No.	cm-1	%T	No.	cm-1	%T	No.	cm-1	%T
1	3868.5	96.9715	2	3750.87	96.1033	3	3644.8	93.5818	4	3345.89	86.3935	5	3055.65	79.669
6	3023.83	69.9296	7	2904.27	83.6932	8	2200.38	97.1121	9	2162.77	96.9423	10	2072.14	97.7583
11	1984.39	97.9836	12	1945.82	94.2286	13	1904.36	92.8141	14	1805.04	94.6612	15	1716.33	84.7078
16	1633.73	60.7616	17	1598.7	69.6326	18	1581.34	53.0487	19	1502.28	61.4996	20	1447.31	78.919
21	1413.57	88.9589	22	1363.43	87.4982	23	1291.11	77.5357	24	1205.29	90.8207	25	1154.19	72.2301
26	1105.01	79.936	27	1071.26	84.4476	28	1013.41	90.9105	29	982.554	60.2227	30	952.662	63.0647
31	915.057	88.0713	32	854.311	81.1127	33	816.706	67.2733	34	776.208	86.3629	35	743.424	47.3317
36	687.498	54.6941	37	607.467	86.47	38	536.114	95.7271	39	507.187	88.7665	40	444.512	96.2973
41	421.37	94.3003	42	410.763	97.2398									

Fig. 3.4.2. IR spectrum of [Co(II)-$(DC)_2$].

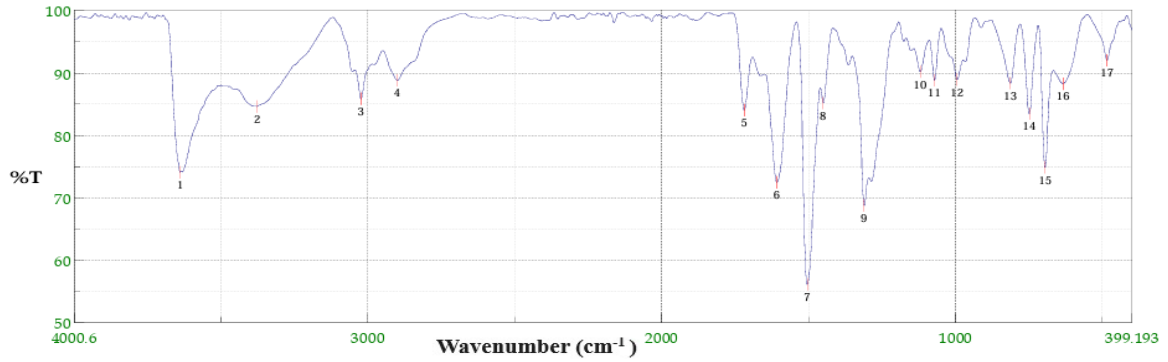

No.	cm-1	%T	No.	cm-1	%T	No.	cm-1	%T	No.	cm-1	%T	No.	cm-1	%T
1	3639.02	74.1036	2	3376.74	84.6451	3	3023.83	85.8543	4	2900.41	88.8354	5	1719.23	84.0447
6	1635.34	72.4785	7	1505.17	56.1327	8	1450.21	85.2054	9	1311.36	68.7722	10	1120.44	90.2033
11	1072.23	88.8216	12	995.089	88.9363	13	813.813	88.3549	14	749.209	83.4953	15	695.212	74.8623
16	634.466	88.2903	17	484.045	92.0448									

Fig. 3.4.3 IR spectrum of [Ni(II)-$(DC)_2$].

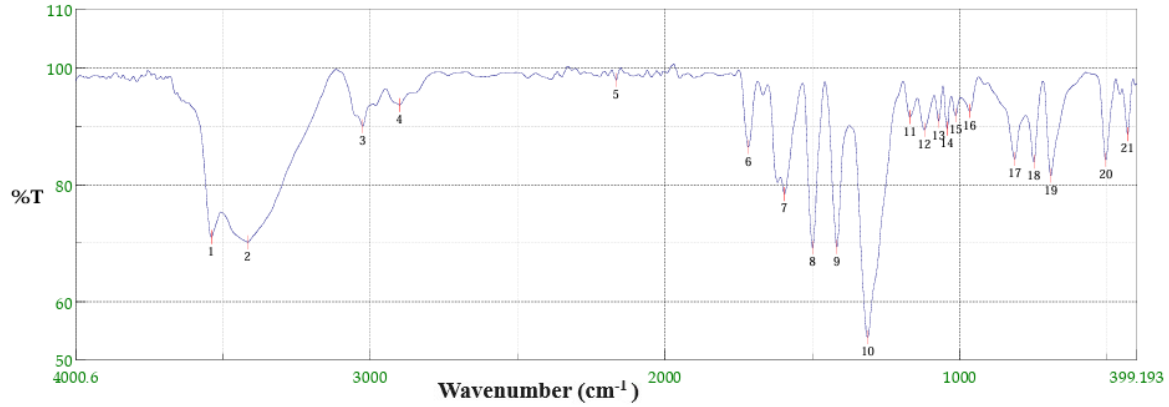

No.	cm-1	%T	No.	cm-1	%T	No.	cm-1	%T	No.	cm-1	%T	No.	cm-1	%T
1	3539.7	71.0378	2	3416.28	70.1876	3	3026.73	90.0546	4	2901.38	93.6798	5	2166.63	97.9988
6	1717.3	86.4933	7	1635.84	78.4402	8	1499.38	69.2463	9	1417.42	69.3676	10	1313.29	53.9268
11	1169.61	91.6171	12	1121.4	89.4295	13	1072.23	90.9578	14	1043.3	89.6577	15	1014.37	91.8765
16	967.126	92.6368	17	813.813	84.4641	18	749.209	83.9834	19	691.355	81.592	20	505.258	84.2756
21	431.012	88.7081												

Fig. 3.4.4. IR spectrum of [Cu(II)-(DC)$_2$].

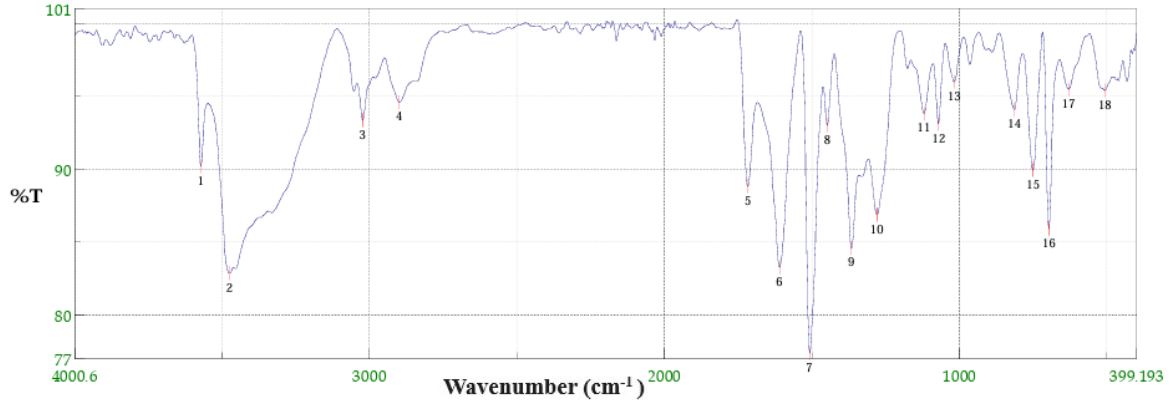

No.	cm-1	%T	No.	cm-1	%T	No.	cm-1	%T	No.	cm-1	%T	No.	cm-1	%T
1	3572.48	90.2194	2	3475.1	82.8794	3	3023.83	93.3856	4	2899.45	94.5925	5	1717.3	88.8235
6	1640.27	83.2986	7	1508.06	77.3843	8	1448.28	93.0217	9	1366.32	84.5991	10	1280.5	86.8911
11	1120.44	93.8505	12	1071.26	93.1366	13	1018.23	96.0128	14	813.813	94.1087	15	751.138	89.9546
16	697.141	85.9252	17	630.609	95.5105	18	487.187	95.4197						

Fig. 3.4.5. IR spectrum of [Zn(II)-(DC)$_2$].

Table 3.4 Important IR spectral bands of DC and complexes.

Compounds	**ν(C=N)**	**ν(M-N)**
DC	1630	-
[Co(II)-(DC)$_2$]	1633	444
[Ni(II)-(DC)$_2$]	1635	484
[Cu(II)-(DC)$_2$]	1635	431
[Zn(II)-(DC)$_2$]	1640	487

3.1.5. ^{1}H NMR spectra

^{1}H NMR spectra of DC and [Zn(II)-(DC)$_2$] were recorded at room temperature in DMSO-d6 solution. ^{1}H NMR spectrum of DC is shown in Fig. 3.5. The ligand, DC displayed a characteristic singlet signal at 8.30 ppm could be assigned to azomethine proton (Refat *et al.* 2014). The observed multiplets in range 7.11-7.67 ppm are attributed to aromatic ring protons (Ali 2014). In the spectrum of [Zn(II)-(DC)$_2$] shown in Fig. 8.7, azomethine proton undergoes deshielding upon coordination and gives singlet signal at 8.40 ppm. This confirms that the coordination took place through azomethine nitrogen. The NMR spectral data further justified the mode of chelation provided by infrared spectral data.

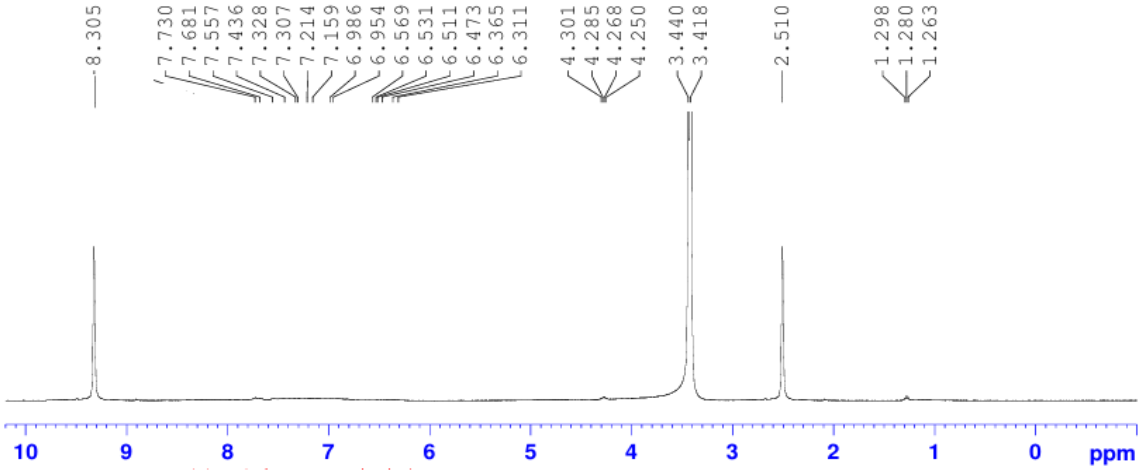

Fig. 9.6 ^{1}H NMR spectrum of DC.

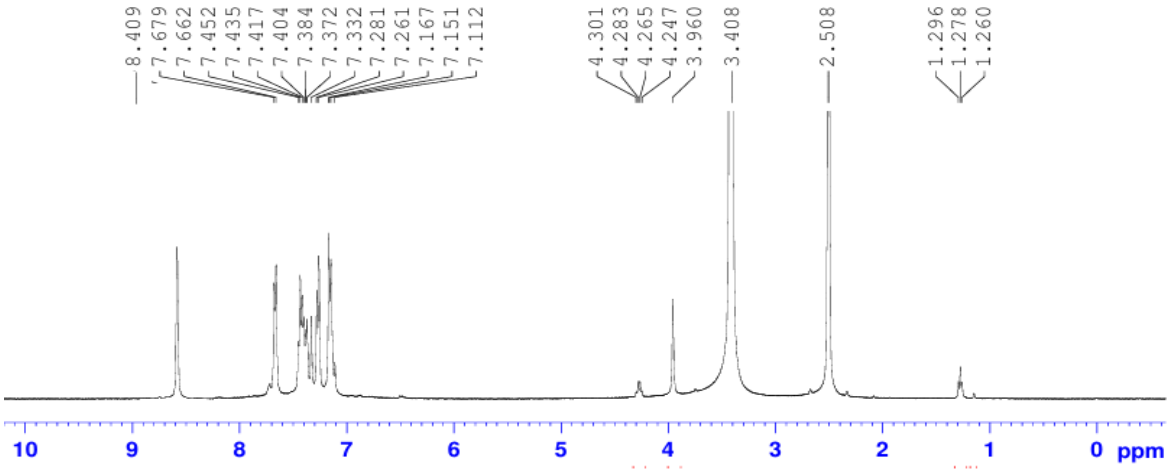

Fig. 9.7 ^{1}H NMR spectrum of [Zn(II)-$(DC)_2$].

3.1.6. UV-Vis. spectrum

An absorption band observed at 315 nm in the UV-Vis. spectrum of DC may be assigned to n–π* transition which is the characteristic of C=N group [Sebastian *et al*., 2011].The position of this spectral band was shifted to higher wavelength region in the spectra of [M(II)-$(DC)_2$] complexes suggesting the coordination of DC to the metal ions.

3.1.7. Electronic spectra

Table 3.7. Electronic spectral data of complexes.

Complexes	**λ_{max} (nm)**	**Transitions**	**Geometry**
[Co(II)-$(DC)_2$]	635	$^{4}A_{2g} \rightarrow {}^{4}T_{1g}$	Tetrahedral
[Ni(II)-$(DC)_2$]	580	$^{1}A_{1g} \rightarrow {}^{1}A_{2g}$	Square planar
[Cu(II)-$(DC)_2$]	640	$^{2}B_{1g} \rightarrow {}^{2}A_{1g}$	Square planar

Electronic spectrum of [Co(II)-$(DC)_2$] showed a band at 635 nm assignable to $^{4}A_{2g} \rightarrow {}^{4}T_{1g}$ transitions in tetrahedral geometrical environment [Dutta & Syamal, 1993]. The observed absorption band in the [Ni(II)-$(DC)_2$] at 580 nm corresponds to $^{1}A_{1g} \rightarrow {}^{1}A_{2g}$ transitions, characteristic of a square planar geometrical environment [Sathyanarayana, 2001]. The broad absorption band detected in the electronic spectrum of [Cu(II)-$(DC)_2$] complex at 640 nm may be accredited to $^{2}B_{1g} \rightarrow {}^{2}A_{1g}$ transition designate square planar geometry. [Zn(II)-$(DC)_2$] complex is diamagnetic and completely filled d^{10} configuration, therefore it would have tetrahedral geometry (Todor & Carmay 2000). The electronic spectral data of complexes are tabulated in Table 3.7.

From the relevant features of spectral data, structure of DC and its complexes are shown in Fig. 3.7.1 (a,b).

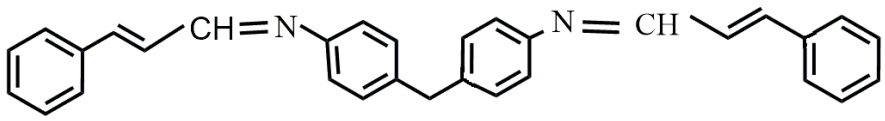

(a)

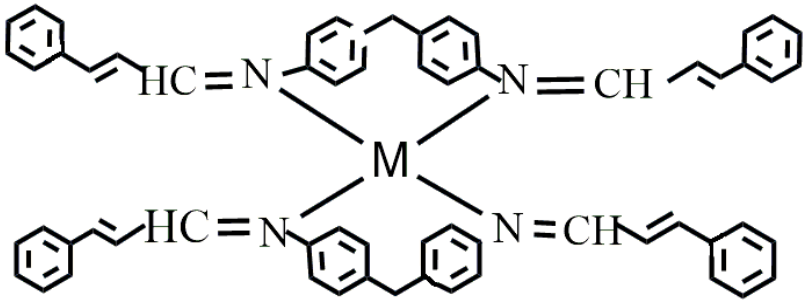

(b)

Fig. 3.7.1. Structure of (a) DC, (b) complexes (M=Co, Ni, Cu & Zn).

3.1.8 Thermal studies

The thermal stability of [Cu(II)-$(DC)_2$] was investigated using TGA analysis at a heating rate of 10˚C min^{-1} in N_2 from 30 to 800˚C. The representative TGA curve of [Cu(II)-$(DC)_2$] is shown in Fig. 3.8. The thermogram of [Cu(II)-$(DC)_2$] clearly shows that there is no weight loss up to 240˚C, indicating stability and the absence of water molecule in the complex. The first stage decomposition observed in the temperature range of 240-250 ºC is attributed due to the melting of ligand. The complex underwent second stage decomposition in the temperature range 350-400 ºC is due to the decomposition of ligand. The complex is being in the form of its metal oxide (Arslan *et al.* 2003) above this temperature.

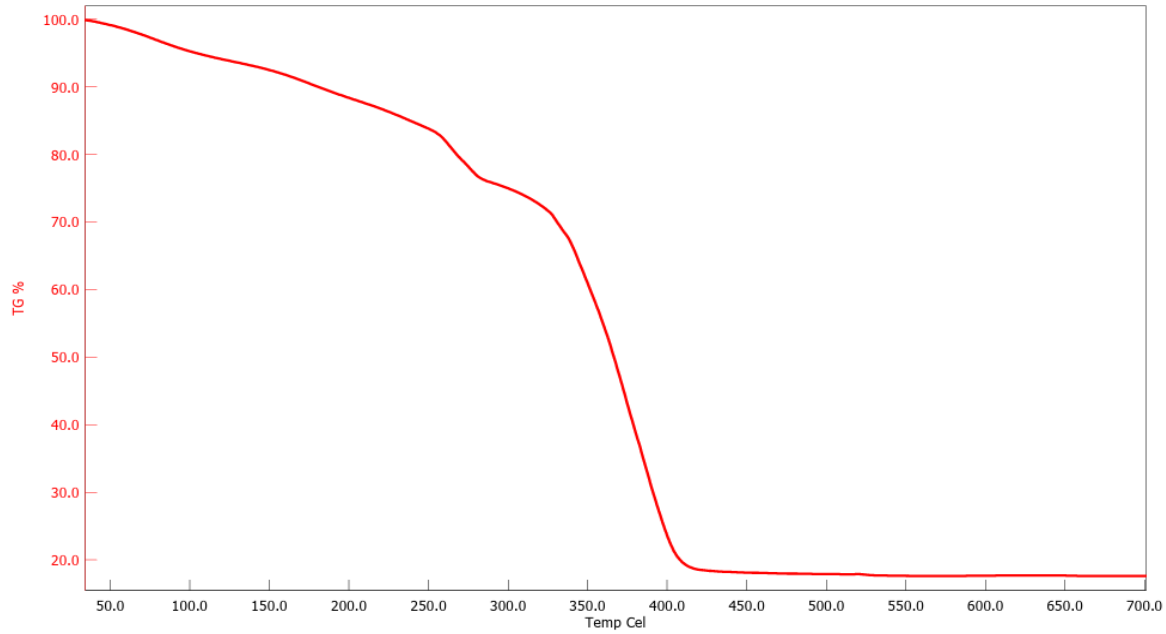

Fig. 3.8. TG of [Cu(II)-$(DC)_2$]**.**

3.1.9. Powder XRD

Powder XRD patterns of DC and [Cu(II)-$(DC)_2$] were recorded over the 2θ = 10˚- 80˚and its patterns are shown in Fig. 3.9. DC showed sharp crystalline peaks could be due to agglomeration and nanocrystalline behaviour of the particles (Cullity 1978). Powder XRD patterns of [Cu(II)-$(DC)_2$] displayed amorphous morphology. Also Debye Scherer's equation was used to calculate the average crystallite size of the ligand and found to be 63 nm suggesting that these samples are in nanocrystalline regime.

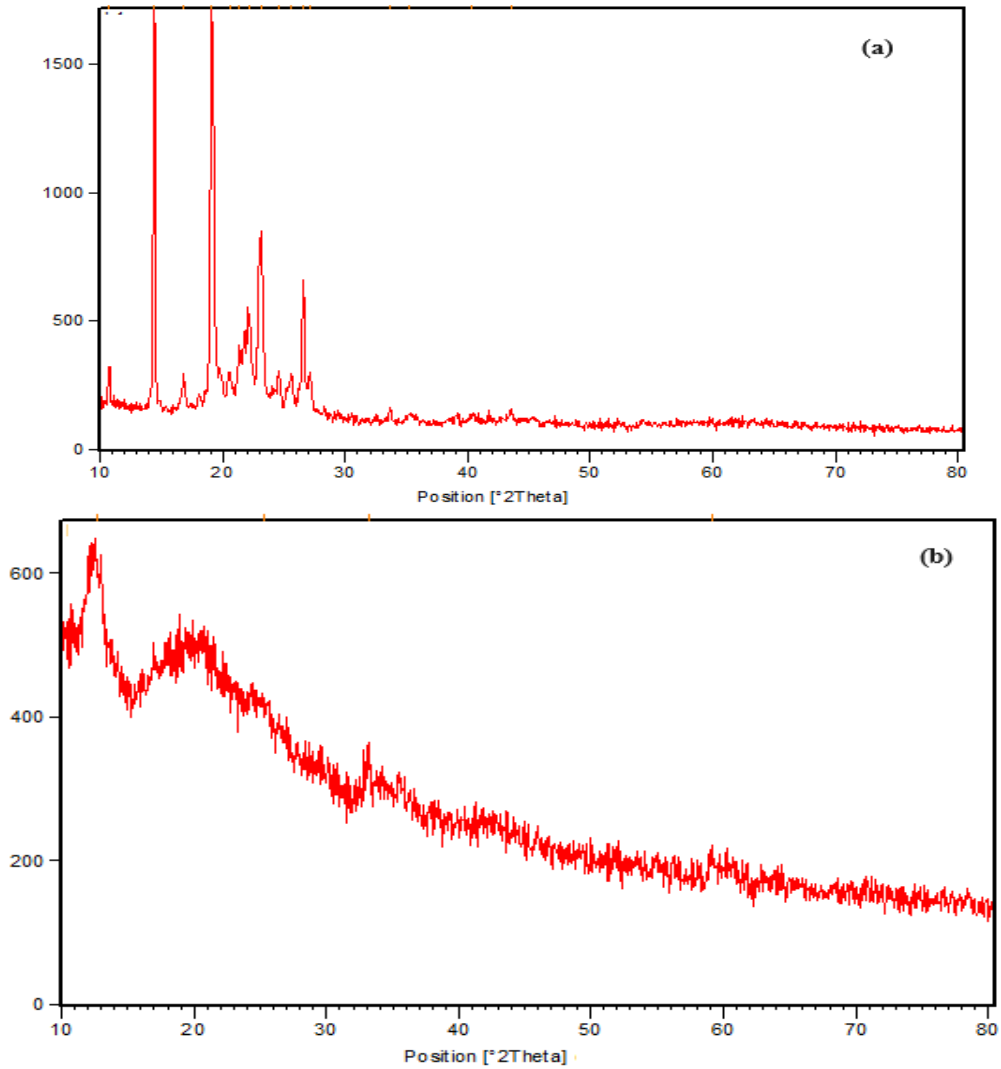

Fig. 3.9. PXRD patterns of (a) DC and (b) [Cu(II)-$(DC)_2$].

3.1.10. SEM

The surface morphology of the DC and its [Cu(II)-$(DC)_2$] complex were studied by scanning electron microscope. The SEM images of DC and its [Cu(II)-$(DC)_2$] are given in Fig. 3.10 (a,b). The SEM image of DC showed flake like surface morphology in nano regime in which particles are randomly distributed (Khan *et al.* 2013). [Cu(II)-$(DC)_2$] complex displayed spherical shape (Joseyphus and Nair 2008).

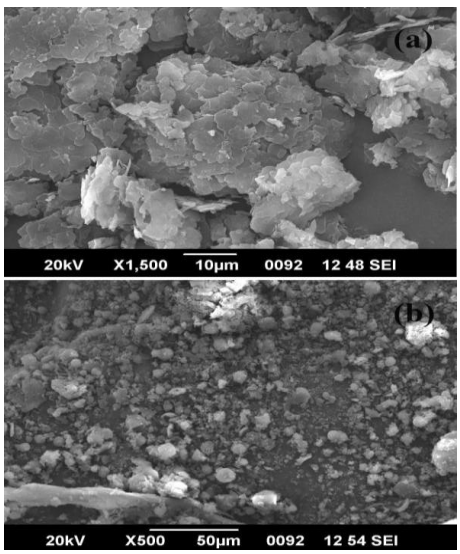

Fig. 3.10(a,b). SEM images of (a) DC and (b) [Cu(II)-$(DC)_2$].

3.2. Biological evaluation

3.2.1 Antimicrobial activity

The plot of variation of inhibition zone of DC and its metal complexes against bacterial and fungal species are shown in Fig. 3.11. *In vitro* antibacterial activity revealed that that ligand and complexes exhibited excellent activities against the tested pathogens, the highest zones of inhibition *i.e*. 22,19, and 24 mm were observed in *Klebsiella*, *A.Niger* and *Pencillium* in case of [Cu(II)-$(DC)_2$], which is even greater than the standard used (Vanomycin). The inhibition zone of synthesized compounds against various tested pathogens is tabulated in Table 3.8.

Table 3.8. Antimicrobial activities of ligand and complexes.

Microbial species		**Zone of inhibition (mm)**					**# Vanomycin /Clotrimazole**
		DC	[Co(II)-$(DC)_2$]	[Ni(II)-$(DC)_2$]	[Cu(II)-$(DC)_2$]	[Zn(II)-$(DC)_2$]	
Bacterial	*Pseudomonas*	12	16	13	15	17	13
	Klebsiella	16	19	20	22	26	15
	S. aureus	10	14	17	21	22	13
Fungal	*C.Albican*	15	18	21	17	24	17
	A.Niger	11	13	10	22	19	18
	Pencillium	13	14	20	18	15	20

Standards

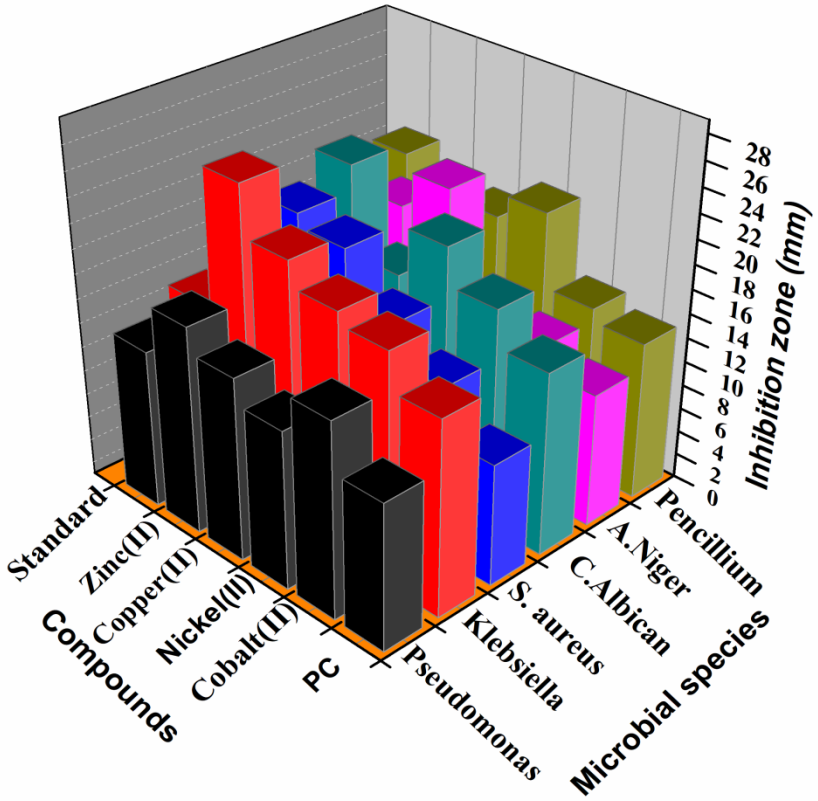

Fig. 3.11. Antimicrobial activity of DC and complexes**.**

Among the complexes, [Cu(II)-$(DC)_2$] complex has maximum and [Zn(II)-$(DC)_2$] complex has least antibacterial effect. For antifungal activity the highest inhibition zone (24 mm) was measured for [Zn(II)-$(DC)_2$] against *C.Albican*. [Ni(II)-$(DC)_2$] showed highest inhibition zone against the fungal species *Pencillium.* In the case of *C.Albican* highest inhibition zone of 24 mm was noted for [Zn(II)-$(DC)_2$]. The antibacterial and antifungal activity of the DC and metal complexes indicate that the complexes possess higher growth inhibition potential than the ligand. The enhanced activities of the complexes are due to the variation in the structure and reactivity of the DC upon coordination (Patil *et al*. 2011).

3.2.2 Antioxidant activity

The radical scavenging effects of ligand and metal complexes at different concentrations were examined and results are summarized in Table 3.9. Concentration dependent plot is presented in Fig. 3.12. It showed that metal complexes have higher activity than the DC, which is mainly due to the coordination of organic ligand with the metal ion. Among the

examined complexes, [Cu(II)-$(DC)_2$] exhibited highest scavenging activity. [Zn(II)-$(DC)_2$] has shown comparable activity. [Co(II)-$(PC)_2$] and [Ni(II)-$(DC)_2$] have shown moderate activity in comparison. The variation in the antioxidant activity results may be due to the redox properties. Generally, chelate ring size, axial ligation, degree of unsaturation in the chelate ring *etc*. are the factors which affect the redox properties of complexes (De Souza and De Giovani 2004).

Table 3.9. Antioxidant activity of DC and complexes.

Compounds	**% Inhibition**			
	250 µg	**500 µg**	**750 µg**	**1000 µg**
DC	7.17	7.58	7.86	8.27
[Co(II)-$(DC)_2$]	11.58	11.72	12.00	12.96
[Ni(II)-$(DC)_2$]	11.44	12.82	13.24	14.34
[Cu(II)-$(DC)_2$]	28.27	28.55	30.34	30.89
[Zn(II)-$(DC)_2$]	23.03	24.00	24.82	25.79

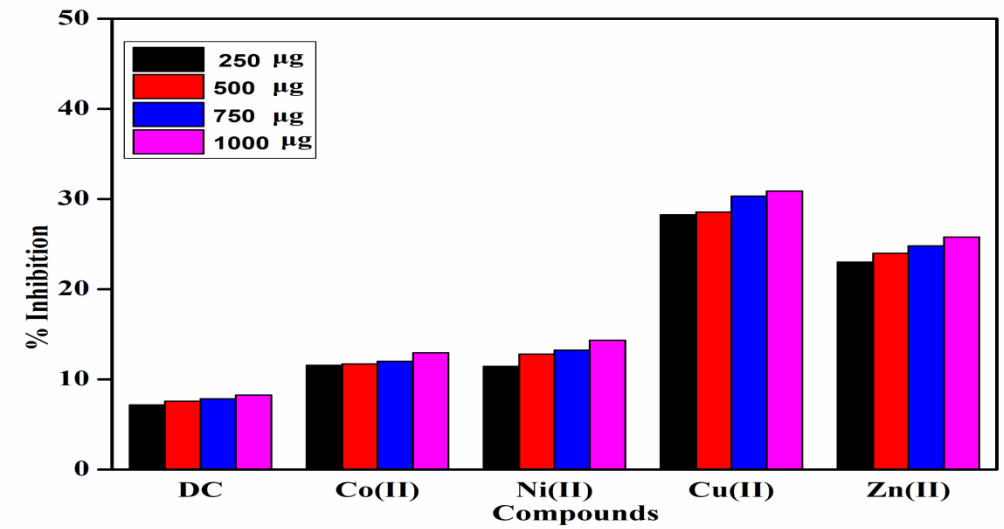

Fig. 3.12. Concentration dependent curves of antioxidant potency of DC and complexes.

3.2.3 Anti-inflammatory activity

Anti-inflamatory activity of DT and complexes are shown in Fig.3.13. The ligand and complexes exhibited effective inhibition of heat induced albumin denaturation at different concentrations as tabulated in Table 3.10.

Table 3.10. Anti-inflammatory activity of DC and complexes.

Compounds	**% Inhibition**			
	25 µg	**50 µg**	**75 µg**	**100 µg**
DC	4.27	4.84	5.22	5.70
[Co(II)-$(DC)_2$]	9.88	11.02	15.20	16.82
[Ni(II)-$(DC)_2$]	15.49	17.11	17.39	18.06
[Cu(II)-$(DC)_2$]	30.89	31.65	33.65	34.41
[Zn(II)-$(DC)_2$]	11.78	12.45	12.64	13.30

The results showed that on increasing the concentration, the percentage inhibition also increased and complexes exhibit higher inhibition capability than that of ligand. The Cu(II) complex showed maximum inhibition of 34.41% at 100 µg/Ml. Ni(II) complex showed 43.15% activity at highest applied concentration. Comparable activity was noted for Co(II) complex, while Zn(II) complex showed least inhibition at the highest concentration.

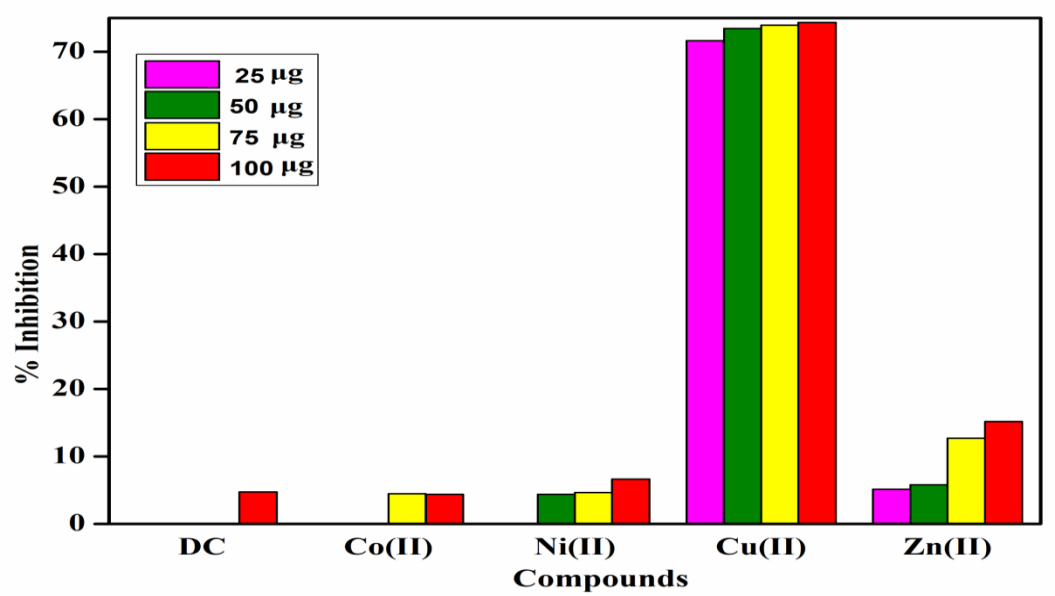

Fig. 3.13. Anti-inflammatory activity of DC and complexes.

3.2.4 Larvicidal activity

The larvicidal activity of DC and metal complexes were performed against the larvae of culex quinquefasciatus at 100 ppm and the result of mortality values are listed in Table 3.11. The graphical representation of larvicidal screening is shown in Figure 3.14. Highest mortality value was observed for Cu(II) complex. Co(II) complex have moderate mortality value against culex quinquefasciatus. Zn(II) complex showed intermediate activity, while Ni(II) complex showed least activity than other complexes. The metal complexes showed higher larvicidal activity than the Schiff base ligand. The increased mortality rate of Cu(II) complex can be due to the increase in lippophilicity on complexation. Chelation increases the liphophilic nature of the central metal atom, within the cell membrane of the larvae and enhancing larvicidal activity of metal complex.

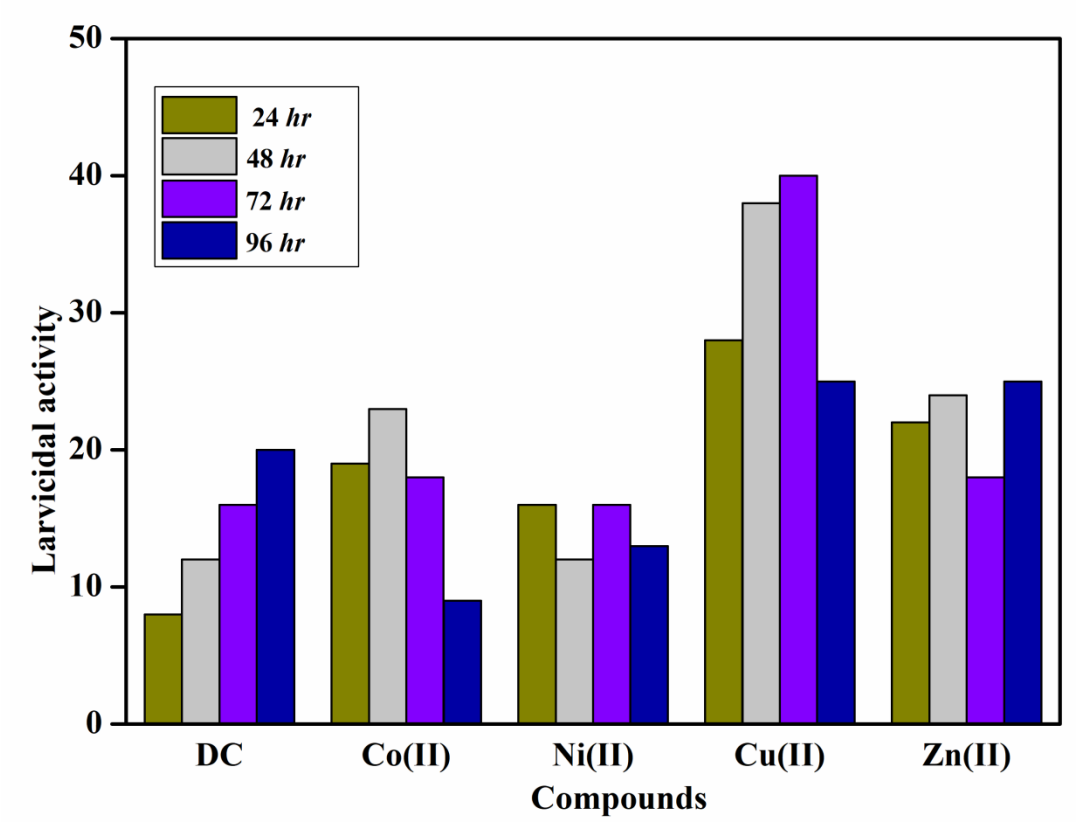

Fig. 3.14. Larvicidal activity of DC and complexes.

Table 3.11. Larvicidal activity of DC and complexes.

Compounds	Larvicidal activity (%)			
	24 hr	***48 hr***	***72 hr***	***96 hr***
DC	8	12	16	20
[Co(II)-$(DC)_2$]	19	23	12	9
[Ni(II)-$(DC)_2$]	16	12	16	13
[Cu(II)-$(DC)_2$]	28	38	40	25
[Zn(II)-$(DC)_2$]	22	24	18	25

3.2.5 Molecular docking

Molecular docking is a preeminent technique in structure-based drug design to understand mechanisms of ligand recognition and specificity and thereby giving an insight into presumable protein-ligand interactions and the binding affinity. Molecular docking studies have been performed to discover the binding mode of the ligand and metal complexes with the most probable site of TP53 (PDB code: 5O1H) (Yan Q *et al*. 2022). Best possible binding sites of DC and complexes are depicted in Fig. 3.15. Docking results are tabulated in Table 3.12.

Table 3.12. Docking results of DC and metal complexes.

Compounds	**Binding free energy (kcal/mol)**	**Bonded Residues**
DC	-4.46	ASP 831, LEU 694, ARG 817
[Co(II)-$(DC)_2$]	-5.75	LEU 889,LEU 820, PHE 771
[Ni(II)-$(DC)_2$]	-5.21	ILE720, LEU753, VAL718
[Cu(II)-$(DC)_2$]	-5.87	SER 816,CYS 773, ASP 831, ASN 868
[Zn(II)-$(DC)_2$]	-5.21	LYS 828, ASP 746, SER 945

In the ligand azomethine nitrogen forms, a bond of 2.5 Å, with LEU 694 residues. The [Co(II)-$(DC)_2$] complex has been docked deeply with the binding pocket of the protein forming two hydrogen bonds with LEU 889 and LEU820 with the binding energy of -5.75 kcal/mol. The ligand and all metal complexes show good binding affinity towards the target receptor. Highest binding affinity has been observed with copper complex and is subjected to in vitro cytotoxicity. The obtained best binding energy of [Cu(II)-$(DC)_2$] complex is -5.87 kcal/mol, while [Zn(II)-$(DC)_2$] had binding energy of -5.21 kcal/mol. Careful examination of molecular docking interactions of [Cu(II)-$(DC)_2$] reveal that the entire metal complex is docked intensively in the groove of the receptor and stabilizes it with hydrogen bonds formed by the amino acid residues SER 816,CYS 773, ASP 831 and ASN 868 (Morris *et al.* 1998).

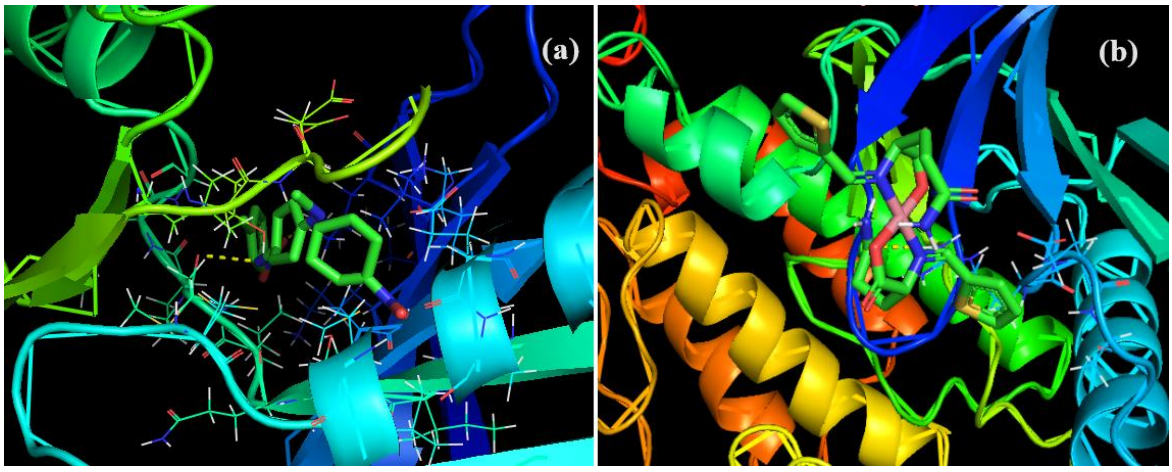

Fig. 3.15. Pictorial representation of binding sites of (a) DC and (b) [Cu(II)-$(DC)_2$].

3.2.6 Cytotoxicity

Cytotoxic and antiproliferative studies using cell lines give relevant information about the anticancer potential of pharmaceuticals. The requirement of anticancer drug candidates is that they should kill the proliferating cancer cells without affecting the normal cells. Here cytotoxicity of [Cu(II)-$(DC)_2$] was evaluated by MTT assay against Saos-2 (bone cancer) cell lines (Pravin *et al*. 2017; Andiappan *et al*. 2018). Dose dependent effects of [Cu(II)-$(DC)_2$] on the cell viability of Saos-2 cell lines are represented in Fig. 3.16. The cell viability at different concentrations are given Table 3.13.
The results indicate that [Cu(II)-$(DC)_2$] exhibited excellent cytotoxic effects at various concentrations, 10 to 100 ug/mL. The curves of [Cu(II)-$(DC)_2$] complex on cell viability of Saos-2 cells illustrated that increase in concentration of [Cu(II)-

$(DC)_2$] adversely decreased the viability of the treated cell lines. Also, highest decrease in cell viability (4.25%) is observed at the highest applied concentration. Cytotoxicity results showed that on increasing the concentration above 75 ug/mL, resulted a drastic change in the morphological characteristics of tested cell lines. Cells become rounded and completely floated in comparison to the control morphology at the highest applied concentration. These results suggest that [Cu(II)-$(DC)_2$] is able to develop an inhibitory effect on the proliferation of the Saos-2 cell line.

Table 3.13. Percentage cell viability of Saos-2 cell lines at different concentrations of [Cu(II)-$(DC)_2$].

Sample concentration (ug/mL)	**Cell viability (%)**
10	88.06
25	86.25
50	84.97
75	72.46
100	4.25
Control (doxorubin)	41.62

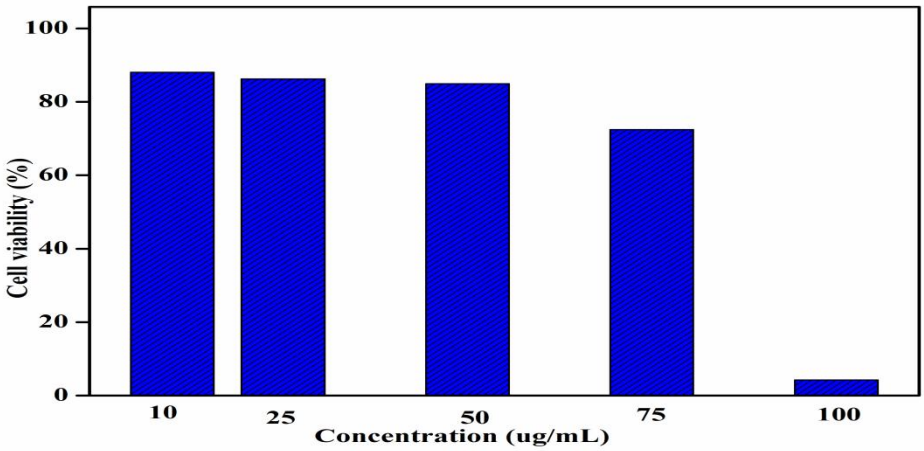

Fig. 3.16. Dose dependent effects of [Cu(II)-$(DC)_2$] on the cell viability of Saos-2 cell lines.

4. CONCLUSIONS

Co(II), Ni(II), Cu(II) and Zn(II) complexes of DC derived from cinnamaldehyde and 4,4'-diaminodiphenylmethane were synthesized and characterized. The results show that ligand is coordinated to the metal ions in a bidentate manner and the geometrical structures of metal complexes are found to be square planar and tetrahedral. Molecular docking studies indicate greater interactions of [Cu(II)-$(DC)_2$] complex with the TP53 evidenced by their best binding energy and highest number of hydrogen bonded residues during interactions. The crystalline nature, crystallite size and morphology have been obtained from PXRD and SEM. Ligand and complexes have exhibited anti-inflammatory and larvicidal activites. The *in vitro* antimicrobial and antioxidant studies revealed that all complexes exhibit significant activities as compared to ligand. The *in-vitro* cytotoxicity studies showed that [Cu(II)-$(DC)_2$] has anticancer activity against bone cancer. Furthermore, [Cu(II)-$(DC)_2$] appears to be an excellent candidate, possessing antioxidant and anticancer activities concomitantly based on the comparative data, hence offering a credible alternative to conventional chemotherapeutic drugs.

5. ACKNOWLEDGEMENT

The authors wish to thank Manonmaniam Sundaranar University, Abishekapatti, Tirunelveli-627 012, Tamil Nadu, India.

6. REFERENCES

1. Arslan, H, Pozan, NO& Tarkan, N 2003, 'Kinetic analysis of thermogravimetric data of p-toluidino-p-chlorophenylglyoxime and of some complexes', Thermochimica Acta, vol.383, pp. 69-77.
2. Cullity, BD 1978, 'Elements of X-ray Diffraction', Addison Wesley, USA.
3. De Souza, RFV& De Giovani WF 2004, 'Antioxidant properties of complexes of flavonoids with metal ions',Redox Report, vol. 9, pp. 97-104.
4. Geary, J 1971, 'The use of conductivity measurements in organic solvents for the characterisation of coordination compounds', Coordination Chemistry Review., vol.7, pp. 81-122.
5. Baradie, KY, El-Wakiel, NA& El-Ghamry, HA 2014, 'Synthesis, characterization and corrosion inhibition in acid medium ofL-histidine Schiff base complexes', Applied Organometallic Chemistry., vol. 29, pp. 117-125.
6. Joseyphus. RS, Dhanaraj, CJ& Nair MS 2006, 'Synthesis and characterization of some Schiff base transition metal complexesderived from vanillin and L(+)-alanine', Transition Metal Chemistry, vol.31, pp. 699-702.

7. Morris, GM, Goodsell, DS, Halliday, RS, Huey, R, Hart, WE, Belew, RK& Olson, AJ 1998, 'Automated Docking Using a Lamarckian Genetic Algorithm and Empirical Binding Free Energy Function', Journal of Computational Chemistry, Vol. 19, vol. 2, pp. 1639-1662.
8. Mohamed GG, Omar MM& Hindy AMM 2005, 'Synthesis, characterization and biological activity of some transition metals with Schiff base derived from 2-thiophene carboxaldehyde and aminobenzoic acid', Spectrochimica Acta A, vol.62, pp.1140-1150.
9. Rezaeivala, M& Keypour, H 2014, 'Schiff base and non-Schiff base macrocyclic ligands and complexes incorporating the pyridine moiety-The first 50 years', Coordination Chemistry Reviews, vol. 280, pp. 203-253.
10. Sebastian, M, Arun, V, Robinson, PP, Leeju, P, Varsha, G, Varghese, D&Yusuff KKM 2011, 'Template synthesis and spectral characterization of some Schiff base complexes derived from quinoxaline-2-carboxaldehyde and L-histidine', Journal of Coordination Chemistry, vol.64, pp. 525-533.